Simulation Analysis on the Blade Airfoil of Small Wind Turbine

Simulation Analysis on the Blade Airfoil of Small Wind Turbine

Hong Zongheng[1], Yu Tao[2] , Chen Guanyu[3] ,Li Xiangrui[4] , Hong Yu[5]

[1,2,3,4,5]Leeds School, SouthWest JiaoTong University, Chengdu City, Sichuan Province, 611756, China

Abstract. The selection of the blade airfoil of wind turbine has a crucial impact on the overall efficiency of wind turbine and wind energy utilization. Aiming at the small 300W household wind turbine on the market, based on its known design parameters and using the software of Profili and SolidWorks, the 3D solid modeling of the blade has been achieved in three common airfoils (NACA4412, NACA0009 and NACA 23012). Then, by using the Fluent module of the finite element analysis software ANSYS, the actual working environment of the blade is simulated. The results show that the blades under the NACA0009 airfoil can produce a relatively maximum axial torque of 3.7808 Nm. Finally, based on the above research method, the new airfoil Icarus was discovered by improving the existing airfoil, which has a relatively low manufacturing cost, and the average pressure difference per unit area of the blade is 4.95% higher than that of the NACA0009 airfoil. This research can provide reference for the improvement of airfoil of small wind turbines, which has certain practical significance and practical value.

1. Introduction

Nowadays, with the depletion and rising prices of traditional energy such as oil, coal, natural gas, more and more attention has been drawn on wind energy as a clean and sustainable energy. From the perspective of development trends, renewable and widely distributed wind energy is huge in its reserves and has the advantage of no pollution, so it will be favored by all countries [1]. Among them, wind power has gradually become the most widely used with its large-scale development conditions and commercial development prospects. By the end of 2016, China's cumulative installed capacity of wind turbines reached 168,732 MW, ranking first in the world[2], and large wind turbines dominated the market. However, in the field of small wind turbines, especially domestic wind turbines, China is still in the development stage compared with developed countries in Europe and America.

Blade technology is the key to the utilization of wind energy, and it is also one of the important breakthroughs in trying to improve the utilization coefficient of wind energy. Blade design includes the choice of airfoil, optimization of chord length and torsion angle distribution, as well as determination of blade thickness to blade chord length[3]. As the component of the wind turbine blade, the airfoil is also the key factor that must be considered when designing the blade. This paper will focus on the selection of small household wind turbine airfoils and 3D modeling of the corresponding blades.

The design parameters of a small wind turbine for household use on the market has been found through the network, and a 3D solid model of the fan blade under different airfoils has been constructed by using the Profili and SolidWorks software. Subsequently, the working environment of the turbine has been simulated by using the Fluent module in ANSYS software, and the finite element

analysis of the force of the three airfoil blades is carried out, aiming at comparing the airfoil selection with the highest efficiency of the wind turbine.

2. Main size parameters of the wind turbine

This paper takes a new type of FD2.2-300W small wind turbine as the research object. This model has been successfully put into production and is actually applied to power generation capacity.

Table 1 FD2.2-300W model small wind turbine design parameters

Wind wheel diameter (D)	number of blades (B)	Blade material	Rated power (P)	Rated power (V_1)	Starting wind speed (V_2)	Wind turbine transmission efficiency ($\eta_1\eta_2$)	Air density (ρ)
2.2m	3	FRP	300W	8.0m/s	3.0m/s	0.85	1.225Kg/m^3

By using the design parameters of the wind turbine described above, combined with the relationship between the diameter of the wind turbine rotor and its output power (as shown in equation (1))[6],

$$D = \left(\frac{8P}{\rho V_1^3 \pi C_p \eta_1 \eta_2}\right)^{\frac{1}{2}} \quad (1)$$

the theoretical wind energy utilization coefficient of this wind turbine can be calculated as C_p=0.296. After removing the diameter of central hub, the radius of the rotor can be assumed to be R = 1.0 m. According to the curve of the wind energy utilization coefficient with the tip speed ratio, the tip speed ratio[4] $\lambda_0 \approx 4.4$ of the wind turbine blade can be obtained.

3. Aerodynamic analysis of the airfoil

The choice of airfoil is important for the efficiency of the wind turbine, which takes into account the factors including blade aerodynamic performance, blade quality and manufacturing difficulty. By consulting relevant data, it is found that the most commonly used and most representative traditional wind turbine airfoil in China is NACA airfoil, so this airfoil family is used as the research blade airfoil[5]. NACA4412, NACA0009 and NACA 23012 are selected for analysis and comparison in the paper. These three airfoils have higher lift-to-drag ratio characteristics in the NACA series, and their research has been relatively mature and fully representative. In this paper, the aerodynamic analysis of the three airfoils NACA4412, NACA0009 and NACA 23012 has been mainly conducted.

Among them, NACA4412 indicates that the relative camber of this type of airfoil is 4%, and the maximum camber position is 0.4 at the length of the chord length, and the relative thickness is 12%. NACA0009 is a classic symmetrical airfoil with a relative thickness of 9%. As for NACA 23012, the first digit indicates that the maximum relative camber of the airfoil is 2/100 = 2%, and the second digit 3 indicates that the position of the maximum relative camber relative to the chord length is 3/20 = 15%. The last three digits indicate that the arc in the airfoil is simple and its relative thickness is 12%[6].

The selection of this airfoil and the calculation of the basic aerodynamic performance of the airfoil are performed by means of Profili software. As an aerodynamic analysis design software specialized in airfoil design and analysis, Profili not only simplifies the selection of the airfoil, but also improves the accuracy of the airfoil design and related aerodynamic calculations, which greatly facilitates the analysis.

The contours of these three airfoils can be derived by using the Profili software, as shown in Figure 1.

Fig. 1-1 The airfoil of NACA4412

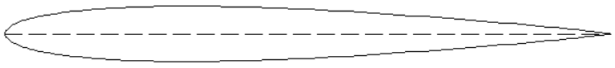

Fig. 1-2 The airfoil of NACA0009

Fig. 1-3 The airfoil of NACA 23012

The most important fluid factor affecting the performance of a low-speed airfoil is the viscosity of the fluid, which indirectly generates lift while directly creating resistance and causes fluid separation. This effect can be directly expressed by the Reynolds number R_e. As the Reynolds number increases, the slope of the lift curve of the airfoil increases, and the maximum lift coefficient increases, and the critical attack angle increases. At the same time, the minimum drag coefficient decreases and the airfoil lift-to-drag ratio increases. Therefore, in the general case (pressure is 101.325 kPa, temperature is 20 ℃, the dynamic viscosity of the air is 17.9×10^{-6} Pa/s), and the air flow rate is the rated wind speed of the wind turbine (V_1 = 8 m/s), the Reynolds number of the air passing through the blades of the wind turbine can be directly expressed as :

$$R_e = \frac{\rho V_1 R}{\mu} = \frac{1.225 \times 8 \times 1}{17.9 \times 10^{-6}} = 5.47 \times 10^5 \quad (2)$$

Using Profili software to analyze the lift-drag ratio of the three airfoils NACA4412, NACA0009 and NACA 23012 under this Reynolds number. As shown in Fig. 2, the relationship between the lift coefficient C_l and the drag coefficient C_d under different airfoil with the attack angle α can be obtained.

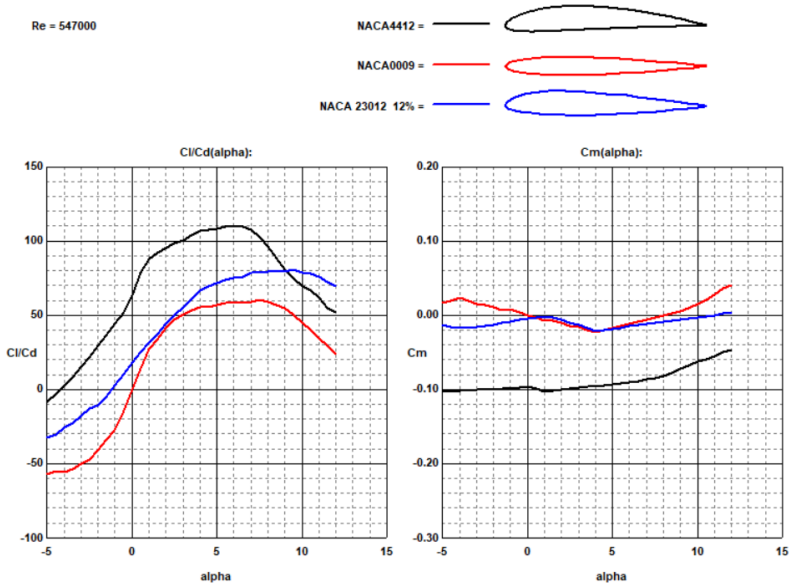

Fig. 2 Variation of the lift-to-drag ratio of the three airfoils with respect to the attack angle α

As can be seen from Figure 2, NACA0009 has a relatively low lift-to-drag ratio. When the attack angle is -5 ° ~ 9 °, NACA4412 has the highest lift-to-drag ratio. When the attack angle exceeds 9°, the NACA 23012 airfoil has the highest lift-to-drag ratio. Therefore, when the attack angle is small, the NACA4412 airfoil has relatively good aerodynamic performance, which is more suitable for the low wind speed start of small wind turbines. In addition, the parameter pairs of these airfoils at the maximum lift-to-drag ratio are shown in Table 2.

Table 2 Comparison of parameters of NACA4412, NACA0009 and NACA 23012 at their maximum lift-to-drag ratio

Airfoil	Best attack angle (α)	Lift coefficient (C_l)	Drag coefficient (C_d)	Maximum lift-to-drag ratio (C_l/ C_d)
NACA4412	6.0	1.0919	0.0099	110.2929
NACA0009	7.5	0.8469	0.0140	60.4929
NACA 23012	9.5	1.1619	0.0144	80.6875

At the same time, under the optimal attack angle of the different airfoils, the static pressure distribution diagram acting on the upper and lower surfaces of the blade are shown in Figure 3:

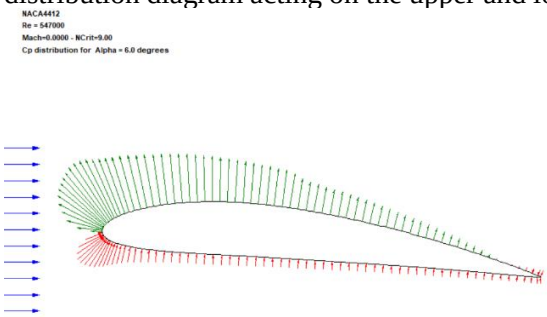

Fig. 3-1 The distribution of Static Pressure on Upper and Lower Parts of NACA4412

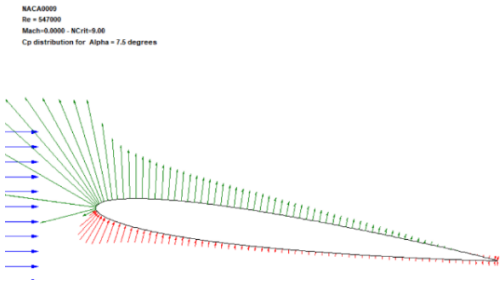

Fig. 3-2 The distribution of Static Pressure on Upper and Lower Parts of NACA0009

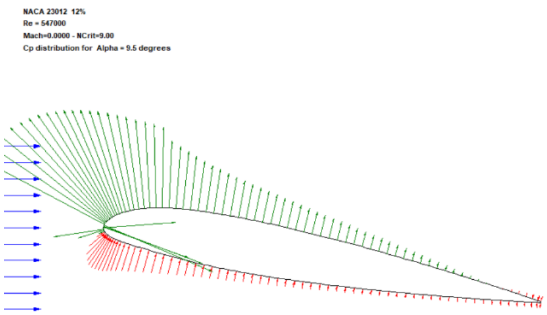

Fig. 3-3 The distribution of Static Pressure on Upper and Lower Parts of NACA 23012

4. Establishment of 3D model of fan blade

4.1 Design idea

According to the Blade-Element theory, the blade is firstly divided into 10 elements, each of which is 0.1R apart. Mainly considering the cooperation between the blade and the hub, the blades at less than 0.1R are designed to be cylindrical, and the blades at 0.2R ~ R are designed with different airfoils (NACA4412, NACA0009 and NACA 23012). By using the Schmitz model and the Glauen vortex theory, the blade model can be simplified to obtain the chord length C and the pitch angle β at different element positions along the radial direction of the blade[8][9]. The specific calculation formulas are as follow:

Tip speed ratio λ_i at the blade rotation radius r_i position:

$$\lambda_i = \lambda_0 \frac{r_i}{R} \tag{3}$$

Ψ use formula

$$\Psi = \frac{(\arctan\lambda_i) + \pi}{3} \tag{4}$$

Axial interference factor k use formula

$$\mathrm{k} = \sqrt{\lambda_i^2 + 1} \times \cos\Psi \tag{5}$$

Tangential interference factor h use formula

$$\mathrm{h} = \sqrt{1 + \frac{(1 - k^2)}{\lambda_i^2}} \tag{6}$$

Inflow angle φ use formula

$$\varphi = \operatorname{arccot}\left(\lambda \times \frac{1 + h}{1 + k}\right) \tag{7}$$

Blade element prime pitch angle β

$$\beta = \varphi - \alpha \tag{8}$$

Calculate the blade chord length C

$$\mathrm{C} = \frac{8\pi r(h - 1)cos\varphi}{BC_l(h + 1)} \tag{9}$$

4.2 Calculation results of blade shape parameters

According to the above formula, by using the MATLAB software to calculate the relevant parameters in Table 1 and Table 2, the aerodynamic characteristics parameters of each section of the blade can be obtained. Taking the airfoil NACA4412 as an example, the calculation results are shown in Table 3.

Table 3 Calculation results of specific dimensions of blades (airfoil NACA4412) on each section

Blade element position /%	Distance from blade root (rotation radius) r/(m)	Tip speed ratio λ_i	Ψ	k	h	φ	Blade element prime pitch angle β	Blade length C
10	0.1	0.44	1.1854	0.4107	2.3008	0.7709	0.6661	0.2169
20	0.2	0.88	1.2877	0.3720	1.4535	0.5661	0.4614	0.2394
30	0.3	1.32	1.3547	0.3551	1.2254	0.4322	0.3275	0.2117
40	0.4	1.76	1.3986	0.3469	1.1331	0.3445	0.2397	0.1803
50	0.5	2.20	1.4286	0.3425	1.0874	0.2844	0.1797	0.1541
60	0.6	2.64	1.4501	0.3399	1.0616	0.2414	0.1367	0.1335
70	0.7	3.08	1.4662	0.3383	1.0456	0.2093	0.1046	0.1172
80	0.8	3.52	1.4785	0.3371	1.0351	0.1845	0.0798	0.1042
90	0.9	3.96	1.4883	0.3364	1.0279	0.1649	0.0602	0.0937
100	1.0	4.4	1.4963	0.3358	1.0227	0.1490	0.0443	0.0850

4.3 Blade modeling based on SolidWorks

Based on the parameter data calculated in Table 3, combined with the specific contour of the airfoil provided in the Profili software, the curve outline of each blade element plane can be drawn by using SolidWorks software as shown in Figure 4.

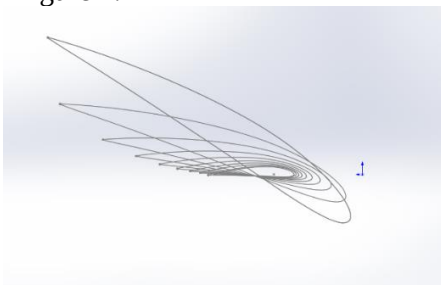

Fig. 4 Sectional view of different blade elements

The 3D solid model of the blade can be successfully constructed by the 'Lofting' command in SolidWorks[10]. The specific results are shown in Figure 5.

Fig. 5-1 3D solid model of NACA4412 airfoil

Fig. 5-2 3D solid model of NACA0009 airfoil

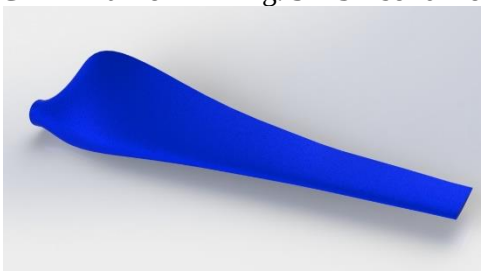

Fig. 5-3 3D solid model of NACA23012 airfoil

5. Finite element analysis of the blade model

Since the actual working environment of the wind turbine is very complicated, and the load acting on the blade is usually cross-linear and random, so it is difficult to calculate the solution by the theoretical formula directly. Therefore, this paper mainly uses the fluid analysis function[11] in ANSYS Fluent to mesh the blade and its airfoil section, aiming at simulating and calculating the static pressure acting on the blade surface and the torque in the direction of the rotating shaft.

Considering that the design requirements of small wind turbines are lower starting wind speeds, the standard k-ω turbulence model for low Reynolds number environment has been selected for simulation analysis of wind turbine blades[12]. In order to improve the simulation accuracy as much as possible, an impeller model was assembled by a reel with the blade model. The tower and other related accessories are neglected, and only the flow field numerical simulation is performed on the impeller model. The calculation domain is a cylindrical region with a velocity inlet and a pressure outlet, where the outlet pressure is the standard atmospheric pressure (1 atm). During the simulation process, the number of grids is 1.61×10^6, and the average quality of the grid is 0.8202. Figure 6 is a schematic diagram of the calculation domain and boundary conditions.

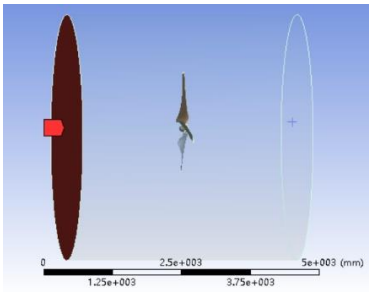

Fig. 6 Computational domains and boundary conditions in the ANSYS Fluent module

5.1 Analysis of aerodynamic characteristics of different airfoils

Figure 7 shows the static pressure nephogram of the blade surface of three different airfoils at the rated wind speed of the wind turbine (V_1=8m/s). Among them, the windward side of the blade is mainly positive pressure (presented in red), and the leeward side of the blade is mainly negative pressure (presented in green).

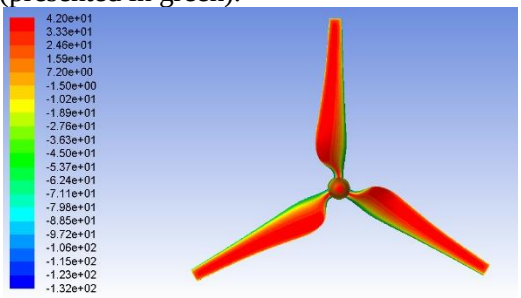

Fig. 7-1 Surface static pressure nephogram of NACA4412 airfoil

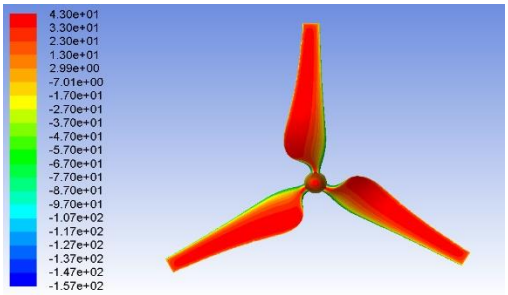

Fig. 7-2 Surface static pressure nephogram of NACA0009 airfoil

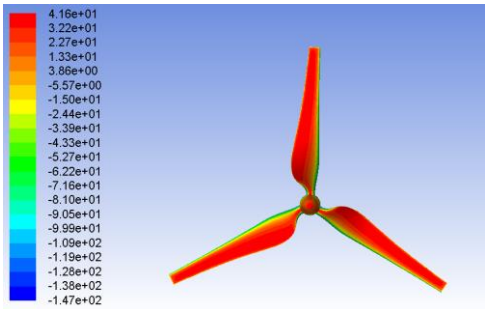

Fig. 7-3 Surface static pressure nephogram of NACA23012 airfoil

By comparing the static pressure cloud charts of impellers with three different airfoils mentioned above, it can be found that the static pressure distribution pattern of the blade surface is almost the same. When the wind turbine is in operation, the maximum pressure is distributed from the tip of the blade to the root of the blade, and the pressure gradually decreases at the trailing edge of the blade.

5.2 Force analysis results of impellers under different airfoils

In order to compare the influence of different airfoils on the force of the fan blades more intuitively, Fluent software is used to calculate the torque on the entire impeller rotation axis (Y-axis) and the blade surface static pressure and other related parameters under the condition of the Reynolds number （$R_e = 5.47 \times 10^5$） and the rated wind speed (V_1=8m/s) in the wind turbine. At the same time, in order to reduce the influence of the difference of the surface area of different airfoil blades on the calculation results as much as possible, the pressure difference on the unit area of the blade has also been briefly explored.

Table 4 Force analysis results of impellers under different airfoils

Airfoil	Total blade area (m^2)	Starting torque (Nm)	Rated torque (Nm)	Maximum positive pressure (Pa)	Maximum negative pressure (Pa)	Average pressure difference per unit area (Pa)
NACA4412	1.0080	0.2453	1.6035	42.2946	-140.5065	6.5827
NACA0009	1.2532	0.5487	3.7808	43.0973	-170.7689	7.0515
NACA 23012	0.9514	0.2900	1.9203	41.6332	-159.6095	6.2215

By comparing the data in the above table, it can be found that the blade of the NACA0009 airfoil have a relatively larger surface area and have a rated axial torque much larger than that of the other two airfoils. Since the axial torque causes the rotation of impeller, the greater the torque indicates, the stronger the ability of the blade to capture wind energy, so the NACA0009 airfoil can maximize the efficiency of the wind turbine. In addition, the upper and lower surface pressure differences per unit area of the NACA0009 airfoil are slightly larger than the other two airfoils, indicating that the airfoil can produce maximum lift.

6. Simulation Analysis of New Airfoil Based on Improved Airfoil

After the above analysis and discussion to determine the comparison method of wind turbine airfoil, it is necessary to explore a new airfoil with better performance. Compared with the three airfoils discussed before, it can theoretically have a higher lift-to-drag ratio while improving the efficiency of the actual operation of the wind turbine. To simplify the difficulty of exploring new airfoils, this paper will focus on improvements to the existing airfoils, especially those which have been analyzed previously. After several simulation attempts, Figure 8 shows the new airfoil Icarus (the mythical characters who used wax and feather to make wings in ancient Greek mythology) improved on the basis of NACA4412 and NACA0009. This new airfoil uses the upper airfoil of the NACA4412, and its lower airfoil is roughly identical to that of the NACA0009. Furthermore, the airfoil can be smoothly transitioned by fine-tuning the coordinates at the intersection of the airfoil. The new airfoil has a maximum thickness of 14.02% at 39.2% of its chord length; its maximum surface is 2.63%, located at 39.2% of the leading edge of the chord. By fitting the coordinates of the upper and lower surfaces of the airfoil, the upper airfoil coordinates are approximated to satisfy the equation: $y_1 = -7 \times 10^{-7}x^4 + 0.0002x^3 - 0.0177x^2 + 0.6893x + 0.8138$. The lower airfoil coordinates are approximated to satisfy the equation: $y_2 = 6 \times 10^{-7}x^4 - 0.0001x^3 + 0.0123x^2 - 0.3985x - 0.4583$

Fig. 8 The airfoil of Icarus

A simple aerodynamic performance analysis of the three airfoils previously discussed (NACA4412, NACA0009 and NACA 23012) and the improved new airfoil (Icarus) is performed by using Profili software. The result is shown in Figure 9.

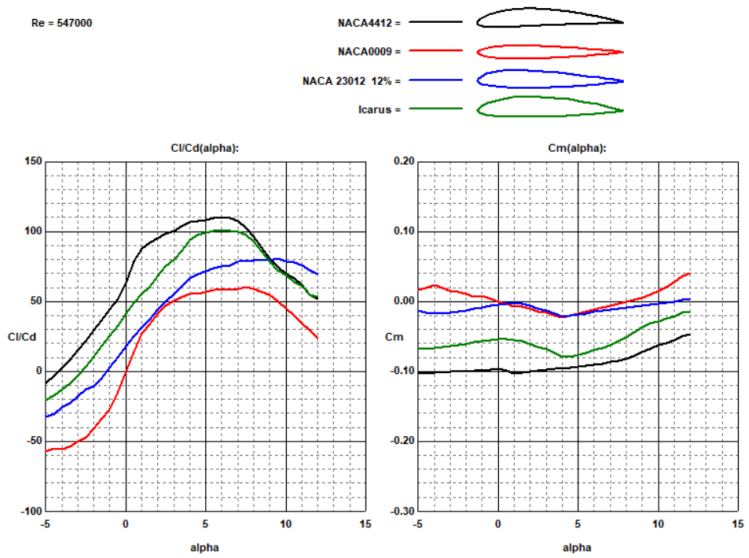

Fig. 9 Variation of the lift-drag ratio of different airfoils with respect to the attack angle α

Through the calculation, in the case of Reynolds number $R_e = 5.47 \times 10^5$, the optimal attack angle of the new airfoil is α=6°, and the maximum lift-to-drag ratio of the airfoil is 101.1111. Combining the relationship curves between the lift-drag ratio with respect to the attack angle α described in Figure 9, it can be found that when the attack angle is less than 9 degrees, the new airfoil has the lift-to-drag ratio second to the NACA4412 airfoil, and then approaches the curve of the airfoil NACA4412.

The improved new airfoil is then imported into the SolidWorks software based on the previously discussed method. According to the specific design parameters of the wind turbine mentioned in Table 1, the solid 3D modeling of the blade of the new airfoil is conducted, and the finite element analysis of the new turbine model is carried out by using the Fluent module in ANSYS software. The simulation results are as follows:

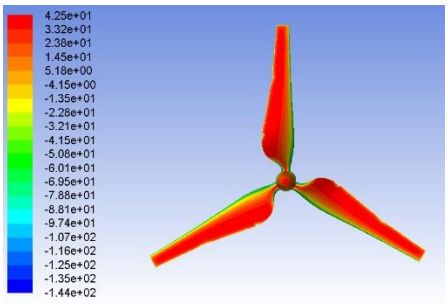

Fig. 10 Surface static pressure nephogram of the new airfoil (Icarus)

Table 5 Simulation results of new airfoil based on ANSYS Fluent

Airfoil	Total blade area（m2）	Starting torque（Nm）	Rated torque（Nm）	Maximum positive pressure (Pa)	Maximum negative pressure (Pa)	Average pressure difference per unit area（Pa）
Icarus	1.0859	0.2939	1.9648	42.5766	-155.3949	7.4005

By comparing the data in Tables 4 and 5, the starting torque and rated torque of the fan blades under the new airfoil (Icarus) are slightly larger than that of the NACA4412 airfoil and NACA 23012 airfoil, while it is smaller than that of the NACA0009 airfoil. However, in the average pressure difference per unit area of the blade, the new airfoil is 4.95% higher than NACA0009 airfoil which is

the most efficient model previously. Make sure that the total area of the blade under new airfoil is slightly smaller than that of the NACA0009 airfoil, it shows that the new airfoil can maximize the working efficiency of the wind turbine at a relatively low cost, and better meet the needs of mass production requirements of small domestic wind turbines.

7. Conclusion

This paper mainly compares the effects of NACA4412, NACA0009 and NACA 23012 on the working efficiency of small wind turbines by constructing the 3D solid model of wind turbine blades and analyzing the aerodynamic calculation of the relevant airfoil. Firstly, the contours of the three airfoils were derived by using Profili software, and their respective optimal attack angle and maximum lift-to-drag ratio were calculated. The NACA4412 airfoil has a relatively larger lift-to-drag ratio of 110.2929 at an attack angle $\alpha=6°$, indicating that the theoretical aerodynamic performance of this airfoil is superior to the other two. Secondly, based on the theory of Blade-Element theory and Glauen vortex theory, the chord length and installation angle of each section of the blade are solved accurately by correlation calculation. Then the SolidWorks software was used to construct the 3D solid models of the fan blade in these three different airfoil cases successfully. Besides, the finite element analysis of the constructed blade models were carried out by using the Fluent module in ANSYS software. The surface area of the NACA0009 airfoil was found to be the largest (1.2532 m^2), and the axial torque was much larger than the other two airfoils (3.7808 Nm). This result shows that the NACA0009 airfoil can maximize the working efficiency of the wind turbine under actual operation. Finally, based on the method summarized above and improving the existing airfoil, a new airfoil Icarus was discovered. This new airfoil has a maximum lift-to-drag ratio of 101.1111, which is second only to the NACA4412 airfoil; the surface area of the blade under this new airfoil is 1.0859 m^2, and the average pressure difference per unit area is 7.4005 Pa, which is 4.95% higher than the NACA0009 airfoil.

References:

[1] W.A. Timmer and R.P.J.O.M. van Rooij, “Summary of the delft university wind turbine dedicated airfoils[J]”. Journal of Solar Energy Engineering, 2003, 125(4): 488－496.
[2] China Industry Information Network, “Analysis on the Status Quo of China's Wind Power Industry Development and Forecast of Future Development Trends in 2018”, http://www.chyxx.com/industry/201803/624700.html
[3] Hu Danmei, Li Jia, et al., “Numerical Simulation of Aerodynamic Performance of Wind Turbine Blade Airfoil”, Renewable Energy Resources, Vol.29, No. 6, Dec.2011
[4] Zhang Renliang, Zhang Junyan, Sun Qin, On 3D modeling and simulation analysis of blade based on Solidworks wind turbine [D]. Hunan: School of Civil Engineering and Mechanics, Xiangtan University, 2013.
[5] Leithead, W. E.， Connor, B.，“Control of variable speed wind turbines: Dynamic models”[J]，International Journal of Control，2000,73（13），1189-1212.
[6] Wang Xueyong, “On Wind Generator Blade Design and 3D Modeling”, Thesis of Master of Engineering, North China Electric Power University, 2008
[7] Zha Jianrui, Yang Yinchuang, Qian Yan, Comparison of multi-wing low-speed aerodynamic characteristics based on Fluent[J]. Hefei: Journal of Hefei Normal University, 2014, 32(6): 38-45.
[8] Yao Xingjia, Tian De, Design and Manufacturing of Wind Turbine [M]. Beijing: Mechanical Industry Press, 2012: 45-67.
[9] Gao Feng, Xu Daping, Lu Yueyi, Modeling of Wind Turbine Wind Turbine Based on Leaf Prime Theory[J]. Modern Electric Power,2007,24(6): 52-57.
[10] Wang Zhide, Cao Yan, Li Yanxia, et al. Modeling method of wind turbine blades based on Solidworks[J]. Inner Mongolia: Journal of Inner Mongolia University of Technology, 2011, 30(2): 129-133.
[11] Ma Peng, Feng Jiahui, Hu Changyang. Calculation of wind turbine airfoil resistance ratio[J].

Huadian Science and Technology. Vol.30, No.7. Jul.2008
[12] Wang Jiyue, Cong Yi, Liang Ning, et al. Bionic design and experiment of small wind turbine blades based on seagull airfoil[J].Jilin: Journal of Agricultural Engineering, 2015, 31(10): 72-77.
[13] M. Borg, M. Collu and F. P. Brennan. Offshore Floating Vertical Axis Wind Turbines: Advantages, Disadvantages, and Dynamics Modelling State of the Art[P]. Cranfield University, UK, 2012.
[14] Ellabban, H. Abu-Rub, F. Blaabjerg. Renewable energy resources: Current status, future prospects and their enabling technology[J]. Renewable and Sustainable Energy Reviews, 2014, 39: 749-763.
[15] J. Cavallo. Wind Energy: Current Status and Future Prospects[J]. Science & Global Security, 1993, 4: 65-109.
[16] E. Benini, A. Toffolo. Optimal Design of Horizontal-Axis Wind Turbines Using Blade-Element Theory and Evolutionary Computation[P]. Department of Mechanical Engineering - University of Padua, Italy, 2002.
[17] S. A. J. Rueda, J. R. P. Vaz. An Approach for the Transient Behavior of Horizontal Axis Wind Turbines Using the Blade Element Theory. Portugal: Science & Engineering Journal, 2014, 24(2): 95-102.